PHYSICAL REVIEW B VOLUME 43, NUMBER 4 1 FEBRUARY 1991

Dynamics of patterns in ferroelastic-martensitic transformations. II. Quasicontinuum model

J. Pouget
Laboratoire de Modélisation en Mécanique, Université Pierre et Marie Curie, Tour 66, 4 place Jusseiu, 75252 Paris CEDEX 05, France
(Received 25 July 1990)

Based on a lattice model describing the elastic phase transition for ferroelastic-martensitic transformations, the set of nonlinear difference-differential equations derived in the preceding paper (I) governs the shearing motion of the atomic layers $(1\bar{1}0)$ stacked in the [110] direction. A quasicontinuum approximation is developed in order to incorporate the leading discreteness effects of the lattice system. The method using the Fourier images of discrete functions leads to a continuum model where macroscopic and microscopic stresses can be deduced from an elastic potential involving a strain gradient. After introducing appropriate boundary conditions on the stresses at each end of the lattice, nonlinear excitations modeling elastic structures are investigated. Then, the quasicontinuum version provides the following results: the existence of (i) quasiperiodic strain waves corresponding to spatially modulated structures, (ii) an array of strain solitary waves representing periodic arrangements of martensitic-austenitic domains, (iii) martensitic or austenitic solitary waves relating to the shearing motions of atomic planes along the stacking direction, and (iv) a static twin interface between martensitic and austenitic domains. The importance of the competing (bending forces) and discreteness effects included in the quasicontinuum model is emphasized to show different regions of existence. Numerical simulations are performed on the microscopic model in order to ascertain the quasicontinuum model and to check the stability of the nonlinear elastic structures. By way of conclusion, comparisons with other works or approaches, as well as extensions of the model, are discussed.

I. INTRODUCTION

The first part of this work (hereafter referred to as paper I, Ref. 1) has been dedicated to a *nonlinear lattice model* for ferroelastic-martensitic transformations. On the basis of a microscopic model[1] we considered a quasicontinuum model in order to describe the *nonlinear patterns* made of *elastic domains* and their dynamics. Martensitic transformations are usually accompanied by elastic twin formation and nucleation of different martensitic variants. Moreover, the dynamics of the twin interfaces are intimately connected with phenomena such as shape-memory effects, for instance. The lattice model built in paper I leads to a set of nonlinear discrete differential equations which are not manageable, so that the quasicontinuum approximation is required and this provides us with an alternative situation making the problem somewhat easier. From the mechanical point of view, we are concerned with the competition between the *nonlocal elasticity* (inhomogeneous deformation) and *local nonlinear elastic energy* (homogeneous states of deformation with stable, unstable, and metastable regions) which plays a crucial role in the motion of coherent elastic structures. In the framework of the present study, we extend the ideas underlying the nonlinear soliton models developed in other contexts[2,3] to the long-wavelength elastic description of twin structures occurring in martensitic transformations. The soliton concept occupies a key position in physics since solitons are elementary nonlinear excitations which allow us to model complex phenomena in nonlinear science. These nonlinear structures in materials range from domain walls in ferromagnetic or ferroelectric crystals[4,5] to incommensurate structures in various media.[6,7]

From the one-dimensional lattice model derived in Ref. 1, we propose to elaborate a continuum approximation with the view of describing nonlinear structures as *martensitic* or *strain solitary waves*. However, a crude approximation to the continuum description leads to erroneous results, especially for dispersion effects which may alter the wave velocity. Therefore, we consider an *interpolation method* which includes the leading discreteness effects due to the lattice system. Such a procedure attempts to describe, at the continuum scale, the lattice dynamics. This produces a quasicontinuum model involving local nonlinear elastic energy and weakly nonlocal strain energy (strain gradient elasticity).[8,9] Then the competition between the nonlocality and nonlinear elasticity plays an important role in the existence of localized structures of the twin boundary type and strain solitary waves can be expected. The model thus built can be compared to the Ginzburg-Landau theory of a first-order phase transition where the order parameter is given by the shear part of the strain tensor in the $[1\bar{1}0]$ direction. However, because of the lattice anisotropy the Landau free-energy expansion includes a third-order term in strain which violates the Landau condition of symmetry.[10–13] In the present work we confine ourselves to a pure shear strain transformation (no dilatation) describing roughly the deformation of a square into a rectangle with preserving area. Such a quasicontinuum model can be applied to alloys such as In-Tl, Fe-Pd, and others

which suffer a cubic-tetragonal ferroelastic transition. Many works have been devoted to martensitic transformations and we can quote the works of Barsch and Krumhansl[14,15] or Mazor and Bishop[16] who established a rather complete model which enables one to calculate the structure of static and dynamic twin boundaries for all temperatures. They place in evidence kink-type solitary twin boundaries between the tetragonal variants of martensite and the cubic high-temperature phase. Mazor and Bishop start with a continuum theoretical Ginzburg-Landau elastic energy functional which involves two strain components in order to describe the structure of twin boundaries in a cubic-tetragonal martensitic transformation. Based on nonlinear lattice dynamics, we propose an alternative, since we have at hand both the microscopic model and its continuum version at this time. This seems to be an interesting direction of investigation because we can define the notion of quasicontinuum where the physical background of the intermediate scale (mesoscale) characterizing the inhomogeneous structure is accounted for.

In order to fulfill the program which has been proposed in this work the basic set of nonlinear difference-differential equations for the microscopic model are recalled in Sec. II, where we describe the physical problem that we want to study. Because the set of discrete nonlinear equations is generally rather difficult to solve we consider the quasicontinuum approximation in Sec. III. The method provides a nonlinear dispersive partial derivative equation where macroscopic and microscopic stresses are defined and derived from an appropriate elastic potential. In addition, the continuum model thus obtained is compared to the general theory of nonlinear elasticity with strain gradient and we can define the correct boundary conditions to close our system. Section IV is devoted to the nonlinear excitation solutions for the quasicontinuum model. We obtain different classes of solutions corresponding to a periodic array of martensitic domains or modulated strain structures. The limiting cases, that is, the martensitic or austenitic solitary waves and martensitic-austenitic kink are examined in Sec. V and numerical simulations are also given in order ascertain the quasicontinuum approximation. For each case, the energy of the system is computed as well as the characteristic size of the nonlinear excitations as functions of the model parameters. At length, some extensions of the lattice model and its quasicontinuum version and also the problem of the complete two-dimensional system are evoked in the conclusion.

II. BASIC EQUATIONS OF THE LATTICE MODEL

Here we recall briefly the lattice model and the basic equations obtained in Ref. 1. These equations have been deduced from a two-dimensional system consisting of square-lattice cells and involving nonlinear and competing interactions. From the lattice energy of the reduced one-dimensional model a set of discrete nonlinear equations has been derived for the discrete deformation which describes the shearing motion of the close-packed atomic planes $(1\bar{1}0)$ along the [110] direction. The special type of competing interactions emerges from the noncentral interactions or bending forces and the lattice potential accounts for the relative displacements as well as the change in angle between bond-segment joining particle pairs. These basic equations are[1]

$$\ddot{S}(n)=\Delta^2[\sigma(n)-\Delta^-\chi(n)] , \tag{1a}$$

where we have defined

$$\sigma(n)=\alpha S(n)-S^2(n)+S^3(n) , \tag{1b}$$

$$\chi(n)=\delta\Delta^- S(n) . \tag{1c}$$

In addition, we have discarded the coefficients β and η which hold for the interactions between the second-nearest atomic planes; this does not change the essence of the physical problem. The index n runs over the [110] direction. Equation (1b) defines the discrete macroscopic stress and Eq. (1c) is the microscopic stress derived from the noncentral interactions or bending forces. Finally, the operators Δ^- and Δ^+ represent the backward and forward first-order finite differences, respectively. From the physical point of view, this set of coupled nonlinear discrete equations (1a) governs the relative shearing motion in the [110] direction polarized in $[1\bar{1}0]$. Because of the strong nonlinear nature of Eqs. (1a)–(1c) we must turn on, here below, the quasicontinuum approximation.

III. CONTINUUM MODEL

A. How to construct the quasicontinuum model

In this section the emphasis is placed especially on the continuum description of the dynamics of the lattice model. The practical problem is how to incorporate correctly the leading effects of the discrete system in a continuum description. This yields us the notion of quasicontinuum which will turn out to be very powerful for our study, but the task is in fact not so easy. The idea is to find a smooth function $u(x,t)$ which is a *good interpolation* of the sampling $[nb,u_n(t)]$ such that $u(x=nb,t)=u_n(t)$. We set up one-to-one correspondence between functions of discrete arguments and a class of *analytical* functions as well as between operations on them. In order to materialize the smoothness condition for $u(x)$ we introduce the Fourier transform $\hat{u}(q)$ of $u(x)$ and we require that $\hat{u}(g)$ differs from zero only on the first Brillouin zone (i.e., $B=[-\pi/b,\pi/b]$) so that the Fourier harmonics with increasing oscillations disappear. This seems to be natural when we deal with lattice problems (see for more details Refs. 17–19).

B. Application to the model

We now propose to apply these ideas to our problem. First of all, we take the Fourier image of Eqs. (1a)–(1c),

$$\omega^2\hat{S}(q,\omega)=4\sin^2(q/2)[\hat{\sigma}(q,\omega)+\delta\sin^2(q/2)\hat{S}(q,\omega)] , \tag{2}$$

where $\hat{S}(q,\omega)$ and $\hat{\sigma}(q,\omega)$ are the Fourier images in space and time of the shear deformation and macroscopic stress whose discrete definition is given by Eq. (1b). But for the latter it is impossible to reach an expression in

terms of $\hat{S}$ since the stress-strain relation is, of course, nonlinear. In order to proceed further, we assume that the discrete functions are slowly varying over the lattice spacing, so that only small-q behavior is concerned. We expand Eq. (2) with respect to q up to the fourth order and multiply by $(1+q^2/12)$ both sides of the equation thus obtained. Upon limiting the expression up to the fourth order, we obtain

$$\omega^2(1+q^2/12)\hat{S}=q^2(\hat{\sigma}+\delta q^2\hat{S}) \ . \tag{3}$$

Now we take the inverse Fourier image of Eq. (3) so that we arrive at the equation for the displacement $V(X,t)$,

$$Q_{tt}=\Sigma_X \ , \tag{4}$$

where we have set

$$Q=V-S_X/12 \ , \tag{5a}$$

$$\Sigma=\sigma(S)-\chi_X \ , \tag{5b}$$

$$S=V_X \ . \tag{5c}$$

Note that $V(X,t)$ and $S(X,t)$ are now the continuous representations of the transverse displacement and shear deformation. In Eq. (5b) Σ is the Cauchy stress, σ the macroscopic stress (as in the classical elasticity), and χ the microscopic stress coming from the noncentral interactions. These stresses derive from an elastic potential as follows:

$$\sigma=\frac{\partial\Phi}{\partial S} \quad \text{and} \quad \chi=\frac{\partial\Phi}{\partial(S_X)} \ . \tag{6}$$

The elastic potential is given then by

$$\Phi(S,S_X)=\tfrac{1}{2}AS^2-\tfrac{1}{3}S^3+\tfrac{1}{4}S^4+\tfrac{1}{2}\delta(S_X)^2 \ . \tag{7}$$

Equation (4) is a nonlinear dispersive partial derivative equation governing the continuous displacement V [or strain if we consider Eq. (5c)]. The nonlinear part is provided by the nonlinear stress-strain relation (nonlinear elasticity) and the dispersive effects are due to the microscopic stress [see Eqs. (6) and (7)]. We note the special form of the inertial term in Eq. (4)—it contains the velocity of the transverse displacement V and the velocity associated with the strain gradient as well. This extra term is caused by the fine description of the discreteness effects in the continuum approximation.

C. Remarks

(i) This continuum approximation can be compared to the more general theory of strain gradient elasticity,[9] but the discreteness effects are obviously absent. Roughly speaking, such a theory tends to introduce the local curvature or the local deformation of the Cartesian frame embedded in the lattice. On the other hand, the microscopic measures how good a nonlocal behavior is to describe lattice bending. The introduction of the gradient becomes efficient when structures in domains and walls are involved.

(ii) The form of the elastic potential (7) corresponds to the Ginzburg-Landau free energy for first-order phase transitions where the shear deformation is merely the order parameter.[10] The elastic coefficient A can be identified to $(C_{11}-C_{12})/2$ (Refs. 20 and 21) (see Sec. V of Ref. 1).

(iii) The equation of motion (4) can be derived from the following Hamiltonian:

$$H=\int_{-\infty}^{+\infty}(K+\Phi)dx \ , \tag{8}$$

where we have defined the density of kinetic energy

$$K=\tfrac{1}{2}(V_t^2+\tfrac{1}{12}S_t^2) \ . \tag{9}$$

It is worthwhile commenting on Eq. (4). This equation contains two types of dispersive terms, which are V_{XXtt} and V_{4X}; if we consider each term separately we obtain two equations of Boussinesq type.[22] Each of them is usually met in the nonlinear dynamics of a lattice[23–25] or in the nonlinear vibrations of elastic beams.[26] However, in our framework the collective contribution of both dispersive terms to the dynamics is of great importance.

(iv) For a finite extended continuum model ($X\in[0, L=(N-1)a]$) it is necessary to introduce boundary conditions at each end of the lattice. Along with the classical elasticity, including the strain gradient, the boundary conditions for the present model read as[9]

$$\begin{aligned}&\Sigma(X=0)=\Sigma_1=T_1 \ ,\\ &\Sigma(X=L)=\Sigma_N=T_N \ ,\end{aligned} \tag{10a}$$

and

$$\begin{aligned}&\chi(X=0)=\chi_1=M_1 \ ,\\ &\chi(X=L)=\chi_N=M_N \ ,\end{aligned} \tag{10b}$$

where the number 1 denotes the first particle [or the first close-packed atomic plane $(1\bar{1}0)$ of the lattice and N is the number of the last particle]. These conditions, written for the one-dimensional continuum model, represent the actions of the surface density force T_1 (T_N) and density torque M_1 (M_N) on the boundaries. We notice that it is important to provide appropriate boundary conditions, especially because they will be useful for the numerical simulations which are, of course, carried out for finite media. Moreover, these conditions must be compatible with the equation of motion (4) by taking Eqs. (5)–(7) into account.

(v) Since we are concerned with a volume-preserving transformation we must check the incompressibility condition. The latter reads as in the (X,Y) coordinate system

$$U_X+V_Y=0 \ . \tag{11}$$

The condition (11) holds true because $U=U_0=$const and V depends only on X (see paper I). Therefore, we do have a martensitic transformation involving only one shear component, namely $S(X,t)$.

(vi) In addition to condition (11) we must add the strain compatibility conditions.[27] Note these conditions make sense only for the continuum model and in the present case they reduce to the single condition

$$S_{XY}=0 \ , \tag{12}$$

which is, of course, satisfied. In fact, the present solution is an exceptional situation, because usually for nonlinear and nonlocal problems of elasticity these compatibility conditions are seldom met. That means that nonlinearities generate incompatibility sources (disclinations, for instance).

IV. NONLINEAR EXCITATION SOLUTIONS

(a) The purpose of this section is to examine the possible existence of nonlinear excitations on the basis of the present lattice model. Then, we must consider the nonlinear equation (4) of the continuum version along with the boundary conditions (10a) and (10b). In addition, we suppose that the surface density torque is zero at each end of the lattice and we choose periodic conditions at each end of the chain. Even if we consider relatively large finite media, these conditions are equivalent to suppose that the specimen is made of periodic arrangements of largely separated twin interfaces. From the mechanical point of view the boundary conditions can be written as

$$\sigma_1-\sigma_N=0\ , \tag{13a}$$

$$\chi_1=\chi_N=0\ . \tag{13b}$$

The first condition involving the macroscopic stress means that the lattice is at the equilibrium while the second condition imposes vanishing microscopic stresses at each end of the lattice. The task of solving Eqs. (4)–(7) with the boundary conditions (13a) and (13b) can be compared to that of the purely continuum model for shape-memory alloys studied by Falk. Some points in Refs. 28 and 29 are different from our lattice model; indeed, the author proposes a one-dimensional Ginzburg-Landau model which fulfills the Landau symmetry. Nevertheless, some results are somewhat very similar, but the dynamics seems to be quite different because of discreteness effects and the nonsymmetrical elastic potential (7).

(b) The simplest idea is to seek solutions to Eq. (4) subject to the conditions (13a) and (13b) as a function of the phase variable $\xi=X-ct$, where c is a constant phase velocity. On putting such a solution into Eq. (4) and by using Eqs. (5a)–(5c) we arrive at

$$c^2Q'=(\sigma-\chi'')'\ , \tag{14a}$$

$$Q=S-S''''/12\ , \tag{14b}$$

where the prime stands for the derivative with respect to ξ. We integrate Eq. (13a) with respect to ξ, then we find

$$c^2Q=\sigma-\chi''+C_1\ , \tag{15}$$

where C_1 is a constant of integration which is determined through the boundary conditions for S_1 and S_N [Eqs. (13a) and (13b)].

From the boundary conditions (13a) and (13b) we can extract three distinct solutions which must be compatible with Eq. (15). (i) A first solution is given by the conditions $S_1=S_N=S_0\neq 0$ at each end of the lattice where S_0 satisfies

$$c^2S_0=\sigma(S_0)+C_1 \tag{16}$$

for a given constant C_1 and $\sigma(S_0)\neq 0$. On the other hand, S_0 can be provided by the equation $\sigma(S_0)=0$ and C_1 is given by Eq. (16) as well. (ii) A second solution represents a martensitic domain embedded in the austenitic phase such that $S_1=S_N=S_0=0$ and in this case Eq. (16) implies $C_1=0$ since $\sigma(0)=0$. (iii) Finally, the particular case $S_1=0$ and $S_N\neq 0$ given by $\sigma_N=0$ implies $c=0$. This particular solution corresponds then to a static austenitic-martensitic boundary interface.

(c) From Eq. (15) and the special form of the stresses [Eqs. (6) and (7)] we arrived at a first integral of the equation of motion

$$\tfrac{1}{2}\gamma(S')^2=W(S) \tag{17a}$$

with

$$W(S)=\tfrac{1}{2}(A-c^2)S^2-\tfrac{1}{3}S^3+\tfrac{1}{4}S^4+C_1S+C_2 \tag{17b}$$

and

$$\gamma=\delta-c^2/12\ , \tag{17c}$$

where C_2 is an integration constant which can be obtained from the boundary conditions. Therefore S' is defined everywhere W is positive. The discussion of the solutions to Eq. (17a) can be qualitatively discussed on the basis of the phase trajectories plotted in the plane (S,S'). Figure 1 shows the trajectories of Eq. (17) for different values of the parameters C_1, C_2, $A-c^2$, and γ. According to the possible roots of (17b), Eq. (17a) leads to unbounded solutions (see curve (a), Fig. 1). In the case where Eq. (17b) has two real roots, we have also unbounded solutions (see curve (b), Fig. 1). Curve (c) in Fig. 1 corresponds to the case where Eq. (17b) has four real roots and bounded periodic solutions exist. Particular cases are obtained when Eq. (17b) has double roots. If Eq. (17b) has one double root, say S_0, solitary waves exist for $S_1<S_0<S_2$ (S_1 and S_2 being the other single roots). Curve (d) in Fig. 1 illustrates this case for $C_1=C_2=0$ and $S_0=0$ (see the Sec. V for more details). Finally, if Eq. (17b) has two double roots, say S_1 and S_2, we have the particular case of the solitary wave corresponding to

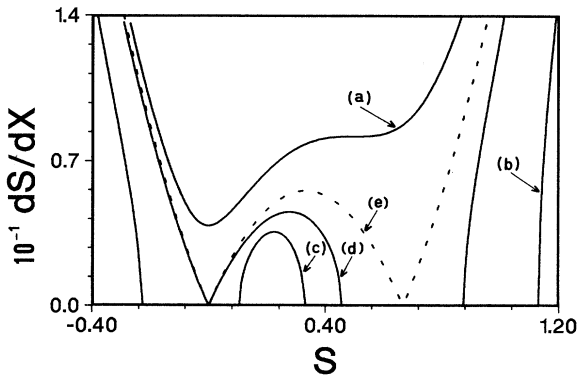

FIG. 1. Phase-trajectory diagram: curves (a) and (b) correspond to unbounded solutions, curve (c) is associated with oscillatory solutions, curve (d) corresponds to the solitary wave solution (see Sec. V A), and curve (e) is the particular case leading to the static domain wall (see Sec. V C).

curve (e) [$C_1=C_2=0$, $A-c^2=\frac{2}{9}$, $S_1=0$, and $S_2=\frac{2}{3}$ in order to satisfy the boundary conditions (13)]. We must have $c=0$ and the solution is static. Since we can get rid of the coefficient γ by changing the variable ξ into $\xi/\sqrt{\gamma}$ if $\gamma>0$, that means that the characteristic width of the excitation is altered by the velocity of the excitation itself. We can say that the faster the propagation the more narrow the excitation. Note that the trajectories have been plotted for $\gamma>0$, but similar results can be obtained for $\gamma<0$.

Numerical simulations of Eqs. (17a)–(17c) show different classes of nonlinear excitations corresponding to some physical situations. Figure 2 sums up the results: Fig. 2(a) gives the strain profile corresponding to curve (c) in Fig. 1. For the latter case we have small oscillations almost sinusoidal about a mean value of S. This leads to a *modulated structure* in the [110] direction. The next figure [Fig. 2(b)] is the situation for which the parameters

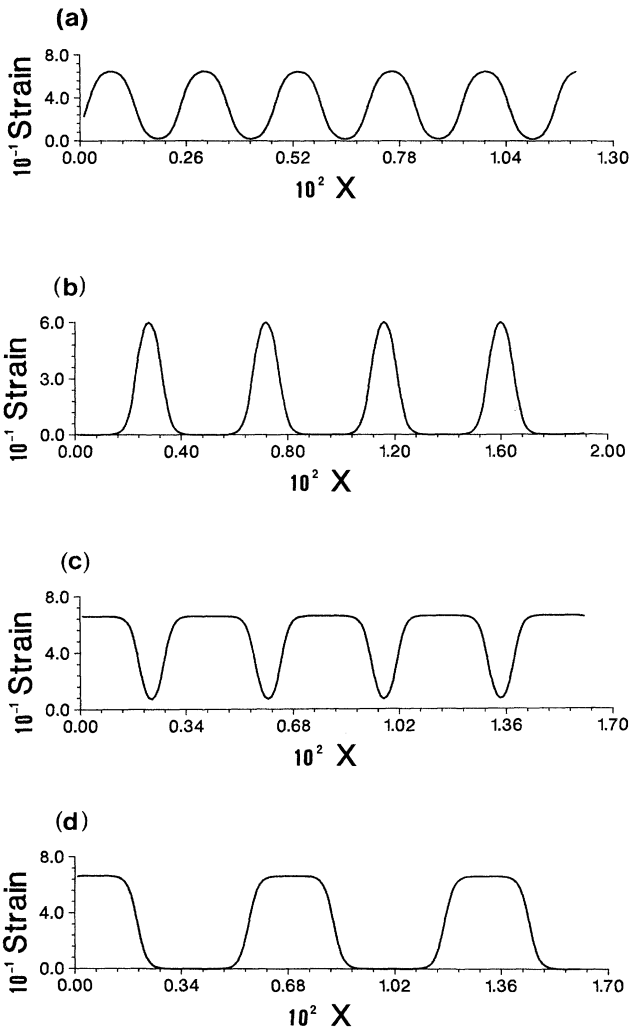

FIG. 2. Some classes of solutions to Eqs. (55a)–(55c): (a) quasisinusoidal solution, (b) array of martensitic solitary waves (nonlinear periodic solution), (c) array of austenitic solitary waves, and (d) array of austenitic-martensitic kink-antikink pairs.

are very close to those corresponding to curve (d) of the phase trajectories (Fig. 1). The strain minimum is nearly zero while the maximum approaches the first single root of curve (d) in Fig. 1. The solution consists of an array of solitons describing a spatially arranged structure made of periodic martensitic and austenitic buffers. The solution can be considered as a *precursor* feature of martensitic transformations and initiates the nucleation of martensitic phases within the parent phase as the transition is approaching.[30] Note, since the period of the modulated strain is continuous with respect to temperature, the precursor effect involves modulations which are *incommensurate* with the parent phase lattice.[15,30,31] We then consider the case where the strain maximum tends towards the double roots of Eq. (17b) and the minimum goes to zero. This situation is illustrated by Fig. 2(c) and periodic austenitic solitons are endowed in the martensitic state. We can characterize this situation as a precursor transformation where the parent phase is partially developed in the martensitic phase. At length, Fig. 2(d) shows an array of kink-antikink pairs when we are very close to trajectory (e) in Fig. 1. This situation represents patterns of rather large martensitic bands. Note some similarities with other models.[28,29]

Section V is devoted to the investigation of the limit cases, that is, when the period of the modulated structure becomes very large. Accordingly, we expect to obtain elastic or strain solitary waves. This situation is somewhat equivalent to studying alloys made of periodic arrangements of largely separated martensitic or austenitic domains.[32,33]

V. STRAIN SOLITARY WAVE SOLUTIONS

A. Martensitic solitary wave

We consider the case where $C_1=C_2=0$ and $S_0\to 0$ which satisfies the boundary condition (16) for $|\xi|$ large enough. According to the trajectories of the phase diagram (curve (d) in Fig. 1), we must have $0<S<S_m$. For this situation an exact solution to (17a)–(17c) can be found

$$S=\frac{S_m}{1+P\sinh^2(Q\xi/2)}\ , \tag{18}$$

where we have set

$$P=\frac{1-3S_m/2}{1-3S_m/4}\ , \tag{19a}$$

$$Q^2=2S_m(1-\tfrac{3}{4}S_m)/3\gamma\ , \tag{19b}$$

where γ is defined by (17c) and it must be positive if $A>0$. The solution (18) depends on S_m which is the maximum strain amplitude and satisfies $W(S_m)=0$. The soliton velocity is strongly dependent on the wave amplitude and is given by

$$c^2=A-\tfrac{2}{3}S_m(1-\tfrac{3}{4}S_m)\ . \tag{20}$$

Nevertheless, the solution (18) is subject to the following constraints on the parameters A, δ, and S_m:

(i) for $\frac{2}{9}\le A\le 12\delta+\frac{2}{9}$ then

$$\sup[0,\tfrac{2}{3}(1-\sqrt{1-9\hat{A}/2})]\le S_m\le\tfrac{2}{3}\ ,$$

(ii) for $0<A<\frac{2}{9}$ then

$$\sup[0,\tfrac{2}{3}(1-\sqrt{1-9\hat{A}/2})]\le S_m\le\tfrac{2}{3}(1-\sqrt{1-9A/2})\ ,$$

(iii) for $A<0$ then

$$S_m<\tfrac{2}{3}(1-\sqrt{1-9\hat{A}/2})\ \text{or}\ S_m>\tfrac{2}{3}(1+\sqrt{1-9\hat{A}/2})\ ,$$

where we have set $\hat{A}=A-12\delta$. The first two conditions guarantee that the velocity is real and we have subsonic waves, whereas the last condition implies only real velocity, since $A\le 0$. We note that the lower limit for conditions (i) and (ii) is zero only if $A<12\delta$. Condition (i) corresponds to the case where the elastic potential $\Phi(S)$ (see Fig. 2 of paper I) has a stable minimum at $S=0$ and metastable minimum at a nonzero strain. However, conditions (ii) and (iii) for $A<\frac{2}{9}$ are associated with the case where the low-temperature or martensitic phase is stable ($S\neq 0$ is the stable minimum of the elastic potential). When S_m approaches zero the soliton velocity is close to that of acoustic-transverse waves. On the other hand, if A is rather large and since S_m is finite, the velocity (20) depends slightly on the wave amplitude; this case corresponds to a linearly elastic behavior. The strain soliton velocity as a function of the amplitude S_m is presented in Fig. 3 for different values of A. Two classes of variation are shown separated by the straight line for $A=\frac{2}{9}$; this special case will be examined in a forthcoming section.

The numerical simulation of the present strain soliton is given in Fig. 4. The numerical scheme is directly provided by the discrete system (1) where the analytic solution (18) is used to provide the initial condition. The illustration represents a small layer of martensite (deformed lattice) moving in the present phase (undeformed lattice). From the physical point of view, the strain soliton corresponds to the dynamics of a strongly distorted lattice layer or a martensitic band sweeping across the crystal in the stacking direction [110]. The corresponding deformed two-dimensional lattice is drawn in Fig. 5.

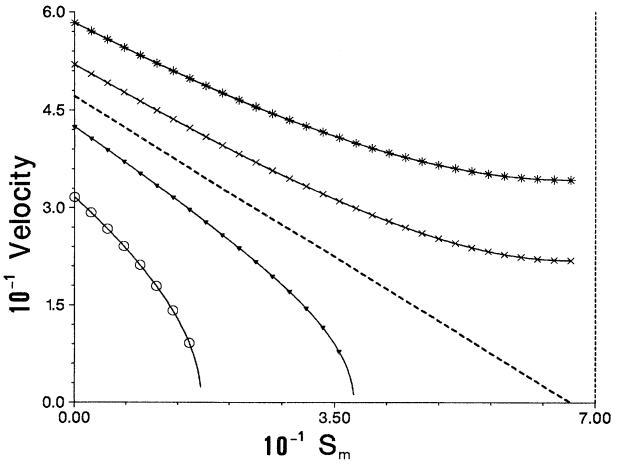

FIG. 3. Martensitic solitary wave: velocity vs strain amplitude for different values of A. The dashed curve corresponds to the particular case $A=\frac{2}{9}$ which splits out the two classes: (○○○), (▼▼▼) for $A<\frac{2}{9}$ and (×××), (***) for $A>\frac{2}{9}$.

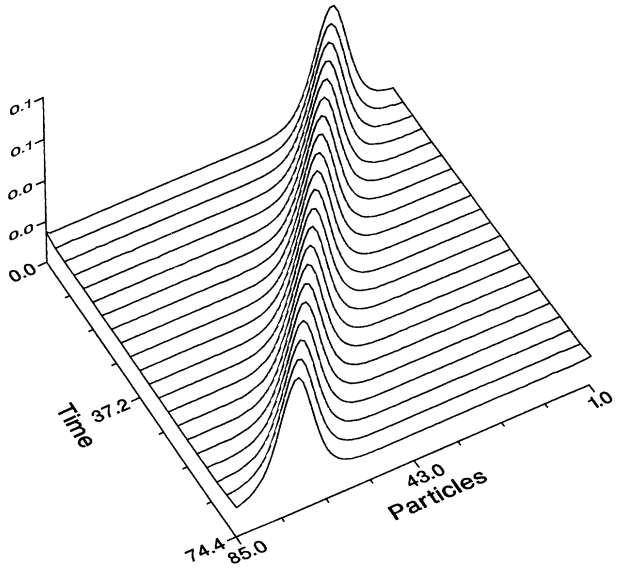

FIG. 4. Numerical simulation of the discrete system: martensitic solitary wave moving on the parent phase ($S=0$).

The total energy of the system is given by the Hamiltonian (8) and after some algebra we find

$$E_{\rm tot}(A,S_m,\delta)=\tfrac{4}{3}\sqrt{2\gamma}\left[\left[c^2+\frac{\delta}{2\gamma}(A-\tfrac{2}{9}-c^2)\right]\times[\tanh^{-1}(\tfrac{3}{2}\sqrt{S_mS_1})]-\left[3c^2+\frac{\delta}{2\gamma}(A-\tfrac{1}{3}-c^2)\right]\times\sqrt{S_mS_1}\right]\ , \tag{21}$$

where we have set $S_1=\frac{4}{3}-S_m$. This energy is plotted in Fig. 6 versus the soliton amplitude for various values of A and δ. We remark that, for whatever $A\le 12\delta$, the total energy can be approximated by

$$E_{\rm tot}\simeq\frac{8\delta}{9}\left[\frac{2}{4(12\delta-A)}\right]^{1/2}(S_m)^{3/2}\ ,$$

when S_m is small enough. Moreover, the energy becomes infinite when γ approaches zero, unless $A=12\delta$ and $E_{\rm tot}$ tends to $-8\delta\sqrt{3}/9$. For $0\le A\le\frac{2}{9}$ the energy is bounded because we must have real velocity, whereas for $A>\frac{2}{9}$ the energy becomes infinite when S_m tends to the upper limit $\frac{2}{3}$. The particular case $A=\frac{2}{9}$ implies that $E_{\rm tot}\to 4\sqrt{2\delta}/81$ when $S_m\to\frac{2}{3}$.

Another quantity is worthwhile examining: the characteristic width of the strain soliton. Since the soliton is a pulselike shape we define the width Δ as the base of the isosceles triangle formed by the tangents to the

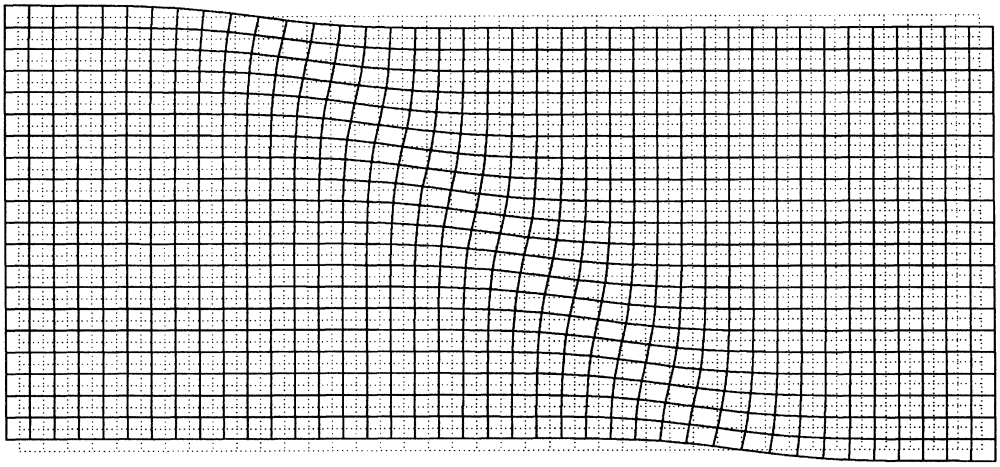

FIG. 5. The associated deformed lattice in the two-dimensional system: strain band along the $[1\bar{1}0]$ direction.

curve at the inflexion points and the ξ axis.

This width is given in Fig. 7. We notice that the thickness is infinite when S_m tends either to 0 or $\frac{2}{3}$ according to the upper or lower limits on S_m due to the conditions of existence. Since the coefficient γ is a function of S_m, then the thickness tends to zero as γ. When S_m is very small that means the harmonic limit of the nonlinear system is valid so that the energy of the system becomes small but the definition of the wave thickness cannot be applied. But if S_m tends towards $\frac{2}{3}$ (only if $A \geq \frac{2}{9}$) the thickness is very large which means that the pulselike soliton is unstable and breaks into a soliton-antisoliton pair. The process, of course, costs much energy which increases. The special case when S_m goes to $\frac{2}{3}$ will be examined for a particular situation.

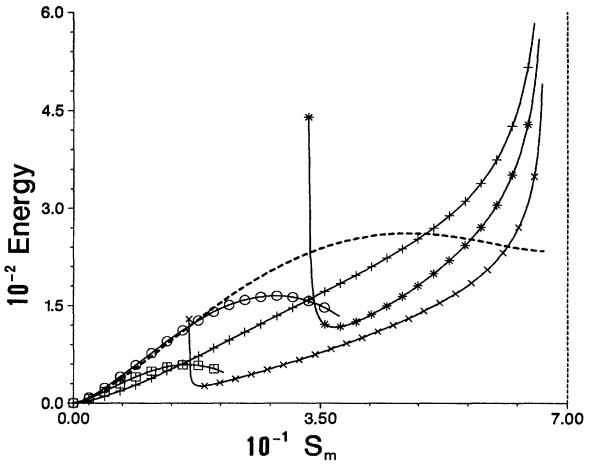

FIG. 6. Martensitic solitary wave: the total energy as a function of the solitary wave amplitude for different values of A and δ. ($\square\square\square$), ($\circ\circ\circ$) for $A < \frac{2}{9}$ and $\delta > A/12$ [condition (ii)], ($+++$) for $A > \frac{2}{9}$ and $\delta > A/12$ [condition (i)], ($\times\times\times$), ($***$) for $A > \frac{2}{9}$ and $\delta < A/12$ [condition (i)], and the dashed line corresponds to the particular case $A = \frac{2}{9}$.

B. Austenitic solitary wave

Another situation occurs when the equation $W(S)=0$ [see Eq. (17b)] possesses a nonzero double root, say S_0, and the right-hand side of Eq. (17a) can be rewritten as

$$W(S)=\tfrac{1}{4}(S-S_0)^2(S-S_a)(S-S_b)\ , \tag{22}$$

where the roots are such that $S_b < S_a < S_0$. The roots S_a and S_b are defined by

$$S_a=\tfrac{2}{3}(1-\tfrac{3}{2}S_0+\sqrt{1-3S_0/2})\ ,$$

$$S_b=\tfrac{2}{3}(1-\tfrac{3}{2}S_0-\sqrt{1-3S_0/2})\ .$$

The study of the existence of such roots leads to

$$\tfrac{1}{2} < S_0 < \tfrac{2}{3}\ . \tag{23}$$

Under the above conditions an analytic solution is found

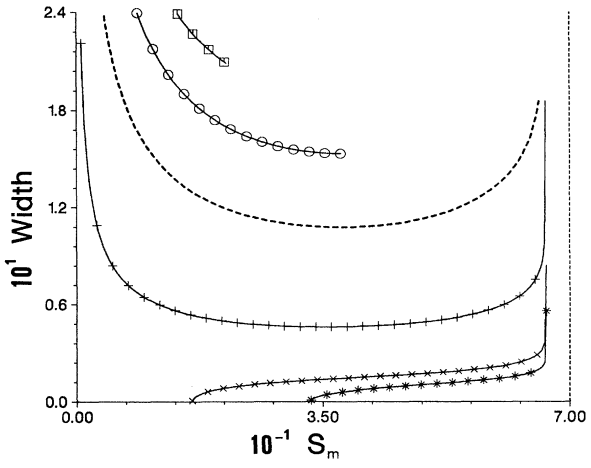

FIG. 7. Martensitic solitary wave: width vs strain amplitude. Note that the width becomes very large when S_m approaches the lower or upper limits of the segment of existence (for caption meaning see Fig. 6).

and it reads as

$$S(\xi)=S_0+\frac{S_a-S_0}{1+2P\sinh^2(Q\xi/2)}\ , \tag{24a}$$

where we have set

$$P=1+(S_0-\tfrac{1}{3})(S_a-S_0)/\gamma Q^2\ , \tag{24b}$$

$$Q^2=S_0(2S_0-1)/\gamma\ . \tag{24c}$$

The wave velocity depends, of course, on the wave amplitude S_0 through the relation

$$c^2=A-S_0(1-S_0)\ . \tag{25}$$

We must have real velocity, whence the additional conditions on S_0 and A:

(i) for $\sup(12\delta+\frac{2}{9},\frac{1}{4})<A<12\delta+\frac{1}{4}$ then

$$\tfrac{1}{2}\le S_0<\tfrac{1}{2}(1+\sqrt{1-4\hat{A}})\ ,$$

(ii) for $\inf(12\delta+\frac{2}{9},\frac{1}{4})<A\le\sup(12\delta+\frac{2}{9},\frac{1}{4})$ then

$$\bar{S}\le S_0<\inf[\tfrac{1}{2}(1+\sqrt{1-4\hat{A}}),\tfrac{2}{3}]\ ,$$

(iii) for $\frac{2}{9}\le A\le\inf(12\delta+\frac{2}{9},\frac{1}{4})$ then

$$\tfrac{1}{2}(1+\sqrt{1-4A})\le S_0\le\tfrac{2}{3}\ ,$$

where we have set $\hat{A}=A-12\delta$ and $\hat{S}=\frac{1}{2}$ if $A>\frac{1}{4}$ or $\bar{S}=(1+\sqrt{1-4A})/2$ if $A\le\frac{1}{4}$. In other cases there is no such solution. The special case $A=\frac{2}{9}$ corresponds to $S_0=\frac{2}{3}$ and $c=0$ which means the wave does not move. In Fig. 8 we have plotted the velocity versus the amplitude S_0 for different A. The first condition (i) can be associated with the case where the elastic potential has only one absolute minimum at $S=0$ (see Fig. 2 of paper I) corresponding to the high-temperature phase because $A>\frac{1}{4}$. Next, the conditions (ii) and (iii) correspond to the metastable minimum at $S\neq0$, but the absolute minimum is still the austenitic phase since $\frac{2}{9}\ge A$. Obviously, for

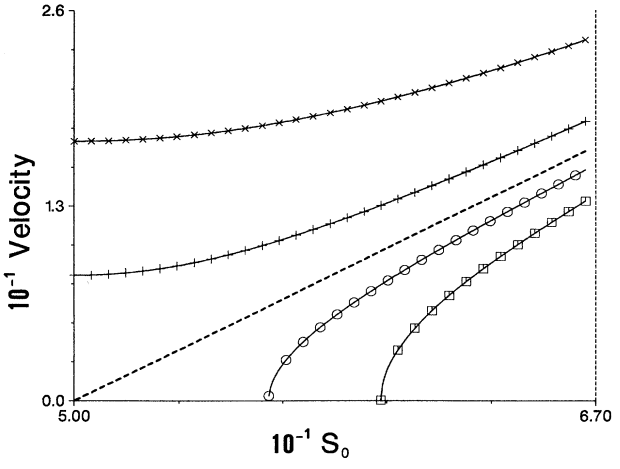

FIG. 8. Austenitic solitary wave: velocity vs strain amplitude for different values of A. The dashed curve corresponds to the particular case $A=\frac{1}{4}$ which separates the two classes: (□□□), (○○○) for $A<\frac{1}{4}$ and (+++), (×××) for $A>\frac{1}{4}$.

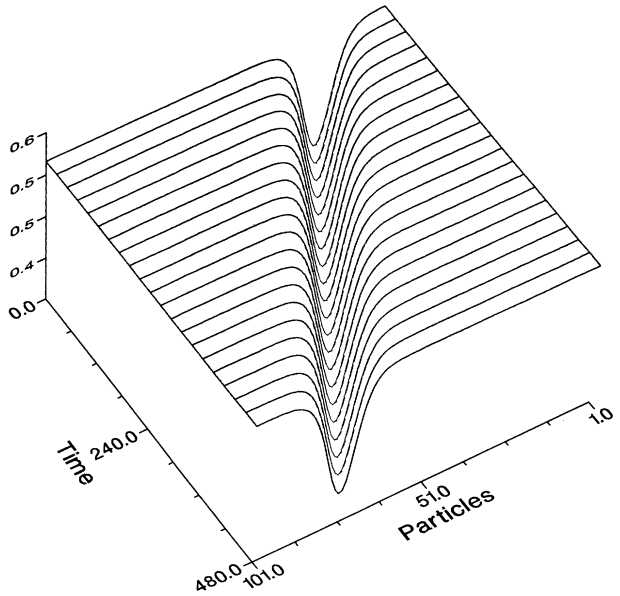

FIG. 9. Numerical simulation of the discrete system: austenitic solitary wave moving on the martensitic phase ($S=S_0$).

$A<\frac{2}{9}$ no solution exists that corresponds to the stable martensitic phase, because the martensitic phase is predominant. We note that for rather small A the wave velocity depends strongly on the amplitude S_0, whereas for a large value of A the amplitude dependence is weak and the crystal behaves almost linearly.

The numerical simulation corresponding to this situation is presented in Fig. 9. As in the previous case the numerical scheme is given by the equations of the discrete model. Figure 9 shows a small layer of austenite (weakly deformed lattice) moving in the martensitic phase. Note that this case is the complementary situation of that of a martensitic domain in an austenitic matrix. In addition, the solution is well defined once the parameter S_0 is known and satisfies the conditions of existence. If we consider the boundary conditions (16a) ($S_0=S_1=S_N$), we remark that $\sigma_1=\sigma_N=\sigma(S_0)\neq0$, unless $c=0$ (i.e., $A=\frac{2}{9}$) because in this particular case S_0 is just the minimum of the elastic potential. If $S_0=\frac{2}{3}$, the strain is constant and equal to S_0.

The total energy of the system is calculated as in the previous case from the Hamiltonian of the continuum model and it is given by

$$E_{\rm tot}(A,S_m,\delta)=-\tfrac{2}{3}\sqrt{2\gamma}\left\{\left[c^2+\frac{4\delta}{\gamma}(A-\tfrac{2}{9}-c^2)\right]\times\left[\tanh^{-1}\left[\frac{\sqrt{S_0S_1}}{S_2}\right]\right]+\left[3c^2+\frac{4\delta}{\gamma}(A-\tfrac{1}{3}-c^2)\right]\times\sqrt{S_0S_1}\right\}\ , \tag{26}$$

where we have defined $S_1=S_0-\frac{1}{2}$ and $S_2=S_0-\frac{1}{3}$. The total energy is expressed in terms of A, δ, and S_0 under the conditions of existence. This energy is plotted versus S_0 in Fig. 10 for various values of A and δ. For S_0 very close to $\frac{1}{2}$ the energy (26) can be approximated by

$$E_{\rm tot}=-6\left[A-\frac{1}{4}-\frac{\delta}{27\hat{\delta}}\right][\hat{\delta}(S_0-\tfrac{1}{2})]^{1/2}\ , \tag{27}$$

with $\hat{\delta}=\delta-(A-\frac{1}{4})/12$. We remark that the energy is infinite when S_0 goes to $\frac{2}{3}$, unless $A=\frac{2}{9}$. For the latter case $c=0$ and $E_{\rm tot}\to 4\sqrt{2\delta}/81$ which is the limit for $S_0=\frac{2}{3}$ [only possible under condition (iii)]. Moreover, the total energy (26) goes to the infinity when γ goes to zero. In Fig. 10 the dashed curve is the limit which separates two classes of solutions when $A\geq\frac{1}{4}$ and $\frac{2}{9}\leq A\leq\frac{1}{4}$, respectively.

The width of the strain soliton is, once again, defined as in the case of the martensitic soliton. This width is plotted in Fig. 11 as a function of S_0. We notice that the lower and upper limits of S_0 depend on A. The width is infinite for $S_0=\frac{1}{2}$ if $A\geq\frac{1}{4}$ and for $S_0=\frac{2}{3}$ if $A\geq\frac{2}{9}$. Moreover, the width tends to zero as the coefficient γ goes also to zero. Note that for $S_0=\frac{1}{2}$ the strain is a constant and the width is obviously very large. The second particular case, namely $S_0=\frac{2}{3}$, corresponds also to a constant solution, unless $A=\frac{2}{9}$, which will be examined. For both limit cases ($S_0\to\frac{1}{2}$ and $S_0\to\frac{2}{3}$) the strain soliton either breaks into a pair of kink-antikink or collapses.

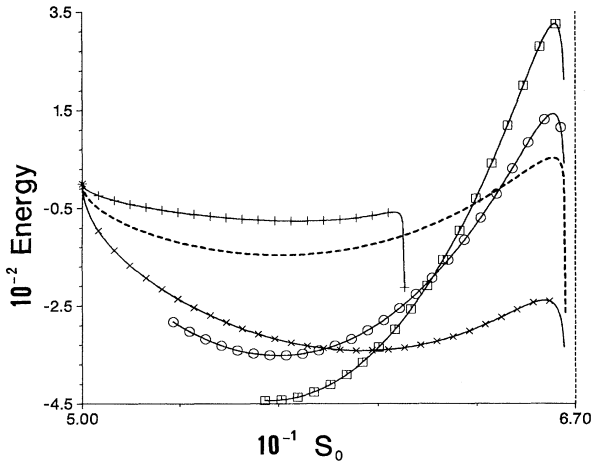

FIG. 10. Austenitic solitary wave: energy as a function of the strain amplitude for different values of A and δ, ($\square\square\square$) and ($\circ\circ\circ$) for $A<\frac{1}{4}$ [condition (ii) or (iii)], ($+++$) for $\frac{1}{4}<A<12\delta+\frac{2}{9}$ [condition (i)], ($\times\times\times$) for $A>\frac{1}{4}$ and $A>12\delta+\frac{2}{9}$ [condition (ii)] and the dashed curve corresponds to the particular case $A=\frac{1}{4}$.

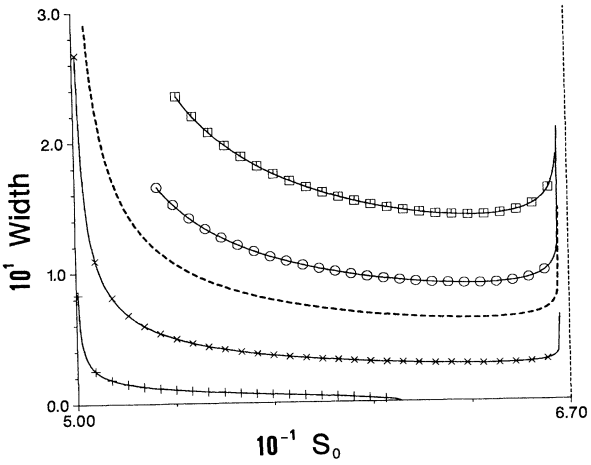

FIG. 11. Austenitic solitary wave: width vs strain amplitude. The width is very large when S_m tends towards $\frac{1}{2}$ or $\frac{2}{3}$ (for caption meaning see Fig. 10).

C. Austenitic-martensitic kink

Now let us examine the particular situation $A=\frac{2}{9}$ which corresponds to curve (e) of the phase-trajectory diagram in Fig. 1. The equation $W(S)=0$ [see Eq. (17)] possesses two double roots if $C_1=C_2=0$ which are $S=0$ and $S=\frac{2}{3}$. Note that we recover the special situation that we have met in Secs. V A and V B. Moreover, if the boundary conditions are considered, the solution must be static since $c=0$. The solution reads as

$$S(X)=\frac{\frac{2}{3}}{1+e^{-QX}}\ , \tag{28}$$

with

$$Q=\tfrac{1}{3}\sqrt{2/\delta}\ .$$

The solution represents a domain wall between an austenitic ($S=0$) and martensitic domains ($S=\frac{2}{3}$). We remark that these two phases have equivalent energies, because for $A=\frac{2}{9}$, $S=0$ and $S=\frac{2}{3}$ are the same minima of the elastic potential (see Fig. 2 of paper I). The solution (28) has been drawn in Fig. 12. The total energy of the system for such a solution is

$$E_{\rm tot}(\delta)=2\sqrt{2\delta}/81\ , \tag{29}$$

and it depends only on δ. The width of the domain wall is then defined by

$$\Delta(\delta)=6\sqrt{2\delta}\ . \tag{30}$$

We notice that the total energy of the system for this case is just twice less than the total energy for the martensitic or austenitic solitary waves when $A=\frac{2}{9}$ and S_m or S_0 goes to $\frac{2}{3}$. This can be explained because for the limiting case the width of solitary waves becomes very big, which means the solution breaks into a kink-antikink pair and the energy of the pair is twice the energy of a single kink.

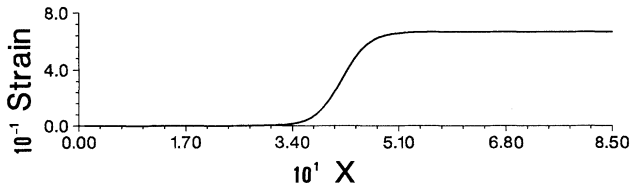

FIG. 12. Case $A=\frac{2}{9}$: static austenitic-martensitic kink between the domains $S=0$ and $S=\frac{2}{3}$.

VI. CONCLUSIONS

In this two-part work we pursued several purposes in order to understand some aspects of ferroelastic-martensitic transformations, such as nonlinear elastic structures or martensitic twinnings. To attack these purposes we first constructed a lattice model including particular interatomic interactions which provided a fine-scale description of microscopic textures made of martensitic domains and interfaces. The model is then appropriate to investigate dynamic problems related to twinning formations. The model can be applied to alloys, such as In-Tl, Fe-Pd, or Nb_3Sn, which suffer a cubic-tetragonal transformation of the first-order type involving shearlike deformations.[12,21]

On the other hand, special attention has been focused on the continuum approximation or the construction of a quasicontinuum, which is a good representation of the lattice including *discreteness effects* (essential if dynamics is concerned). The method uses the *Fourier image* of the discrete quantities, and by assuming the long-wavelength approximation we are able to transform the differential-difference equations, which are usually not exactly solvable, into a partial derivative equation. This procedure turns out to be very appropriate for our problem. Nevertheless, works concerning a quasicontinuum description of anharmonic atomic chains have been discussed; these works use different concepts, including higher-order corrective terms,[34] incorporating leading discreteness effects,[24,25] or developing iterative methods in order to calculate very narrow solitary waves as accurately as possible.[35] Note that all the methods developed assume *a priori* that we can find analytical functions which are good approximations of the discrete quantities; however, the method fails if a very discrete nature of the model is essential. For instance, domain wall pinning, incommensurate structures, or transition to chaos due to particular competing interactions at the microscopic scale cannot be described by quasicontinuum approximation, accurate though it was. Our quasicontinuum procedure leads to two dispersive terms in Eqs. (4) and (5a)–(5c): the term V_{4x} is due to the noncentral forces and it is inherent to the model itself; the other term V_{xxtt} represents the leading discreteness effects. The two terms can produce competing effects and they can modify deeply the nature of the nonlinear excitation; indeed, the coefficient γ defined by (17c) depends on the wave velocity. On the other hand, solitary wave solutions contain γ so that the thickness of the strain soliton is very dependent on the velocity. Moreover, the collective effects of the noncentral interaction, discreteness effects, and nonlinearities can cause drastic unstable phenomena or very interesting dynamic problems. These aspects of the model will be undertaken in another work.

Some results of the present model can be compared to works relating to martensitic transformations often based on the continuum point of view, especially insofar as martensitic solitary wave descriptions are concerned.[14–16,28,29] The present model can be also compared to another lattice model which has been developed to study martensitic patterns, but for this one-dimensional model a lattice energy expansion up to the sixth order in strain has been considered. However, similar results concerning strain solitary waves have been obtained.[36]

The original part of the present study lies in the construction of a model at two scale levels: microscopic and quasicontinuum, which enables one to present the following results: (i) the propagation of nonlinear excitations describing the shearing motion of the atomic planes $(1\bar{1}0)$ along the stacking direction [110] representing spatially arranged structures made of periodic martensitic domains and referred to as "tweed" patterns[30,31,37,38] and (ii) the existence of strain solitary waves of a martensitic or austenitic type. The domain patterns corresponding to our localized strain structures are commonly observed by means of electron microscopy or other means in various alloys such as Ni-Ti, Ti-Mn, In-Tl, etc.[32,33] Some numerical estimates can be computed from available experimental data for the In-Tl alloy.[20,21,39] We then obtain a width of martensitic domains about 8–10 lattice spacings, which is commonly observed on high resolution electron microscopy.[32,33]

Nevertheless, further extensions of the model are worthwhile investigating both in the discrete model and its quasicontinuum approximation. We can study, for instance, the very discrete problem of the nonlinear structures without passing to the continuum approximation. This problem can be tackled by looking for the states which minimize the lattice energy, leading thus to the ground state. This question seems to be very appropriate in the case of rather tiny martensitic domains and microtwinnings. In order to understand the mechanism of domain nucleation and lattice stability we must consider a complete two-dimensional system; this allows one to examine *localized elastic domains* and their *stability* or the formation of very rich domain patterns.[40] These interesting problems will be proposed elsewhere. It seems to be important to investigate the influence of an external field and damping on the dynamics of such structures. However, it has appeared to us that the one-directional problem was quite essential to pave the way for studies of more complex systems and the one-dimensional model is a good guide for selecting the pertinent phenomena.

ACKNOWLEDGMENTS

The Laboratoire de Modélisation en Mécarique is Unité Associée au Centre National de la Recherche Scientifique.

[1]J. Pouget, preceding paper, Phys. Rev. B **43**, 3575 (1991).
[2]A. R. Bishop, J. A. Krumhansl, and S. E. Trullinger, Physica D **1**, 1 (1980).
[3]A. R. Bishop, Phys. Scr. **20**, 409 (1979).
[4]F. H. De Leeuw, R. Van Den Doel, and U. Enz, Rep. Prog. Phys. **43**, 683 (1980).
[5]A. Fouskova and J. Fousek, Phys. Status Solidi A **32**, 213 (1975).
[6]H. Shiba and Y. Ishibashi, J. Phys. Soc. Jpn. **44**, 1592 (1978).
[7]P. Bak, Rep. Prog. Phys. **45**, 587 (1982).
[8]J. A. Krumhansl, in *Lattice Dynamics,* edited by R. F. Wallis (Pergamon, Oxford, U.K., 1963).
[9]R. D. Mindlin and N. H. Eshel, Int. J. Solids Struct. **4**, 109 (1968).
[10]J. C. Toledano and P. Toledano, *The Landau Theory of Phase Transitions* (World Scientific, Singapore, 1987).
[11]P. W. Anderson and E. I. Blount, Phys. Rev. Lett. **14**, 217 (1965).
[12]J. K. Liakos and G. A. Saunders, Philos. Mag. A **46**, 217 (1982).
[13]J. Pouget, Phase Transition **14**, 251 (1989).
[14]G. R. Barsch and J. A. Krumhansl, Phys. Rev. Lett. **53**, 1069 (1984).
[15]G. R. Barsch and J. A. Krumhansi, Metall. Trans. **19A**, 761 (1987).
[16]A. Mazor and A. R. Bishop, Phys. Rev. B **40**, 5084 (1989).
[17]L. Briouillin, *Wave Propagation in Periodic Structures* (Dover, New York, 1953).
[18]J. A. Krumhansl, in *Mechanics of Generalized Continua,* edited by E. Kröner (Springer-Verlag, Berlin, 1982).
[19]I. A. Kunin, *Elastic Media with Microstructure. I. One-Dimensional Models,* Vol. 26 of *Springer Series in Solid-State Sciences* (Springer-Verlag, Berlin, 1982).
[20]D. J. Gunton and G. A. Saunders, Solid State Commun. **14**, 865 (1974).
[21]M. P. Brassington and G. A. Saunders, Proc. R. Soc. London Ser. A **387**, 289 (1983).
[22]A. C. Scott, F. Y. F. Chu, and D. W. McLaughlin, Proc. IEEE **61**, 1443 (1973).
[23]St. Pnevmatikos, in *Proceedings of the International Conference on Singularities and Dynamical Systems,* edited by Sp. Pnevmatikos (North-Holland, Amsterdam, 1985).
[24]Ph. Roseneau, Phys. Lett. A **118**, 222 (1986).
[25]Ph. Roseneau, Phys. Rev. B **36**, 5868 (1987).
[26]M. P. Soerensen, P. L. Christiansen, and P. S. Lomdahl, J. Acoust. Soc. Am. **76**, 871 (1984).
[27]C. Teodosiu, *Elastic Models of Crystal Defects* (Springer-Verlag, Berlin, 1982).
[28]F. Falk, Z. Phys. B **51**, 177 (1983).
[29]F. Falk, Z. Phys. B **54**, 159 (1984).
[30]Y. Yamada, Y. Noda, M. Takimoto, and K. Furukawa, J. Phys. Soc. Jpn. **54**, 2940 (1985).
[31]L. E. Tanner, A. R. Pelton, and R. Gronsky, J. Phys. (Paris) **43**, C4-169 (1982).
[32]K. M. Knowles, J. M. Christian, and D. A. Smith, J. Phys. (Paris) **43**, C4-185 (1982).
[33]S. Kajiwara and T. Kikuchi, Philos. Mag. A **48**, 509 (1983).
[34]M. Collins and S. A. Rice, J. Chem. Phys. **77**, 2607 (1982).
[35]D. Hochstrasser, F. G. Mertens, and H. Buttner, Physica D **35**, 259 (1989).
[36]J. Pouget, in *Physical Properties and Thermodynamic Behavior of Minerals,* Vol. 225 of the *NATO Advanced Studies Institute Series C: Mathematical and Physical Sciences,* edited by E. K. H. Salje (Reidel, Dordrecht, 1988), pp. 359–401.
[37]R. Oshima, M. Sugiyama, and F. E. Fujita, Metall. Trans. **19A**, 805 (1988).
[38]S. M. Shapiro, in *Competing Interactions and Microstructures: Statics and Dynamics,* Vol. 27 of *Springer Proceedings in Physics,* edited by R. LeSar, A. Bishop, and R. Heffner (Springer-Verlag, Berlin, 1988), pp. 84–94.
[39]Y. Murakami, J. Phys. Soc. Jpn. **38**, 404 (1975).
[40]J. Pouget, in *Continuum Models and Discrete Systems 6,* edited by G. A. Maugin (Longman, London, 1990).